A COMPARISON OF POROUS STRUCTURES ON THE PERFORMANCE OF SLIDER BEARING WITH SURFACE ROUGHNESS IN MICROPOLAR FLUID FILM LUBRICATION

by

Pentyala Srinivasa RAO*, Birendra MURMU, and Santosh AGARWAL

Department of Applied Mathematics, Indian Institute of Technology (ISM),
Dhanbad, India

Original scientific paper
https://doi.org/10.2298/TSCI170825304R

This paper presents the theoretical analysis of comparison of porous structures on the performance of a slider bearing with surface roughness in micropolar fluid film lubrication. The globular sphere model and Irmay's capillary fissures model have been subject to investigations. The general Reynolds equation which incorporates randomized roughness structure with micropolar fluid is solved with suitable boundary conditions to get the pressure distribution, which is then used to obtain the load carrying capacity. The graphical representations suggest that the globular sphere model scores over the Irmay's capillary fissures model for an overall improved performance. The numerical computations of the results show that, the act of the porous structures on the performance of a slider bearing is improved for the micropolar lubricants as compared to the corresponding Newtonian lubricants.

Key words: *surface roughness, porous, pressure, slider bearing, micropolar fluid*

Introduction

The slider bearing is simplest, among the hydrodynamic bearings and frequently encountered because the expression of film thickness is simple and boundary conditions to be required zero at the bearing ends are not that complicated. Self-lubricated porous bearings, such as sintered bearings in which pores are impregnated with oil, are extensively used in industrial applications such as in instruments, domestic appliances, audio-visual equipment's, business machines, industrial machines, automobiles, and small electric motors. In addition to these, their low cost makes them economically viable. The development of the theory of hydrodynamic lubrication of porous bearings is not new. The Morgan and Cameron [1] were first gave an analytical survey of study of the porous bearings with the aid of hydrodynamic conditions. There have been numerous studies of various types of porous bearings, such as slider bearings by Uma [2], journal bearings by Prakash and Vij [3], and thrust bearings by Gupta and Kapur [4]. In all these studies the lubricant was Newtonian fluid. However, the Newtonian fluid constitutive approximation is not a satisfactory engineering approach to most of the lubrication problems. Hence the use of non-Newtonian fluids as lubricants has gained its importance in the modern industry. The experimental result shows that the addition of a small amount of long-chain polymer solutions (paraffin family) to a Newtonian fluid gives the most desirable lubricant. The study of the effect of surface roughness has a greater importance in the study of porous bearings as the surface roughness is inherent to the process used in the manufacturing industries. In general,

*Corresponding author, e-mail: pentyalasrinivasa@gmail.com

the roughness asperity height is of the same order as the mean separation between the lubricated contacts. In the situations, surface roughness affects the performance of the bearing system and it is inevitable to consider the influence of surface roughness on over all loads carrying mechanism. The micro-continuum theory is the simplest generalization of the classical theory of fluids, which allows for the polar effects such as the presence of micropolar fluids and body couples. The micropolar fluids might the expected to appear to a noticeable extent in a lubricant containing long-chain molecules when it is confined to narrow passages. Further, micropolar fluid theory is also the generalisation of classical theory of fluids [5]. However, in general due to non-uniform rubbing of the surface especially in slider bearing the distribution of surface roughness may be asymmetrical. Andharia *et al*. [6] studied the effect of surface roughness on the performance characteristics of 1-D slider bearings with an assumption of the probability density function for the random variable characterizing the surface roughness is asymmetrical with a non-zero mean.

The problems of slider bearings have received considerable attention as these are amenable to easy mathematical analysis. Such bearings are used for supporting transverse loads. The analysis of slider bearings with various film shapes is done by Pinkus, Sternlitcht, [7] and Hamrock [8] for Newtonian lubricants based on the assumption of perfectly smooth bearing surfaces. It is well known that the bearing surfaces, particularly after having some run-in and wear develop roughness. Several theories have been proposed for the study of surface roughness effects. The effect of 2-D sinusoidal roughness on the load support characteristics of a lubricant film was studied by Burton [9]. Tzeng and Saibel [10] introduced a stochastic concept for the study of 1-D surface roughness on the performance of 2-D inclined slider bearings. A more general form of dynamic Reynolds equation for micropolar fluid lubrication of porous slider bearings has been derived by Naduvinamani and Marali [11]. The generalized form of Reynolds equations have been derived by Christensen [12] and Elrod [13]. All these studies have been confined to non-porous bearings. In the case of porous bearings the problem of studying the effect of surface roughness is of greater importance, as the surface roughness is inherent in the process of their manufacture. The stochastic theory developed by Christensen for the hydrodynamic lubrication of rough surface has been extended for the porous bearings by Prakash and Tiwari [14]. Siddangouda *et al*. [15] proposed the study of combined effects of micropolarity and surface roughness on the hydrodynamic lubrication of slider bearings by mathematically modelling the surface roughness by a stochastic random variable with non-zero mean, variance and skewness. Advantages and disadvantages of traditional and modern approaches of surface analysis based on concepts of roughness and texture were discussed.

None of the research article mentioned in the literature have consider the influence of different porous structure and the realistic applications, it is necessary consider in industrial application like oil recovery, piston rings and so on. The purpose of the present work is to consider different porous structures on the performance of slider bearings with surface roughness in micropolar fluid film lubrication.

Mathematical formulation of the problem

Figure 1 shows the geometry and physical configuration of the porous inclined slider bearing. It consists of two surfaces separated by a lubricant film. The lower surface of the porous bearing is at rest and the upper solid surface is moving in its own plane with a constant velocity, U. The minimum film thickness is h_0 and maximum h_1. It is assumed that the bearing surfaces are rough and infinitely wide in the z-direction. The lubricant in the film region as well as in the porous region is assumed to be micropolar fluids.

To represent the surface roughness the mathematical expression for the film thickness is considered to be consisting of two parts:

$$H(x) = h(x) + h_s \tag{1}$$

where $h(x)$ is the mean film thickness, h_s, is a randomly varying quantity measured from the mean level and thus characterizes the surface roughness, and L_1 is the length of the bearing. Further, stochastic part h_s is considered to have the probability density function $f(h_s)$ defined over the domain, $-C \le h_s \le C$, where C is the maximum deviation from the mean film thickness. The mean α^*, the standard deviation σ^* and the parameter ε^*, which is the measure of symmetry of the random variable h_s, are defined:

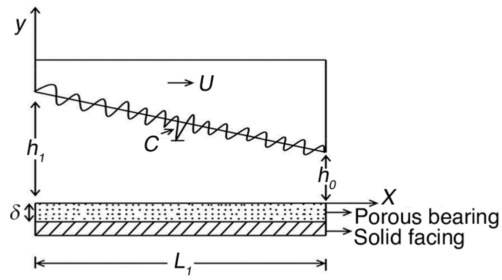

Figure 1. Porous slider bearing system

$$\alpha^* = E\,(h_s) \tag{2}$$

$$\sigma^{*2} = E\,[(h_s - \alpha^*)^2] \tag{3}$$

$$\varepsilon^* = E\,[(h_s - \alpha^*)^3] \tag{4}$$

where E is an expectancy operator defined by:

$$E(\circ) = \int_{-\infty}^{\infty} (\circ)\, f(h_s)\, \mathrm{d}h_s \tag{5}$$

where the parameters α^*, σ^*, and ε^* are all independent of x. The mean α^* and the parameter ε^* can assume both positive and negative values, whereas σ^* always assumes positive values. It is assumed that the lubrication in the film region and that in the porous region is an incompressible fluid. It is also assumed that the body forces and body couples are absent.

The characteristic coefficients across the film of the micropolar fluid are constant. The basic equations governing the flow of micropolar lubricants under the usual assumptions of lubrication theory take the form.

Conservation of mass:

$$\frac{\partial u}{\partial x} + \frac{\partial v}{\partial y} = 0 \tag{6}$$

Conservation of linear momentum:

$$(\mu + K)\frac{\partial^2 u}{\partial y^2} + K\frac{\partial v_1}{\partial y} - \frac{\partial p}{\partial x} = 0 \tag{7}$$

$$\frac{\partial p}{\partial y} = 0 \tag{8}$$

Conservation of angular momentum:

$$\gamma\frac{\partial^2 v_1}{\partial y^2} - 2Kv_1 - K\frac{\partial u}{\partial y} = 0 \tag{9}$$

where u and v are the fluid velocity components in the x- and y-directions, respectively, and v_1 (x,y) is the micro-rotational velocity component, p – the fluid pressure, μ – the Newtonian viscosity coefficient, K and γ are additional viscosity coefficients for micropolar fluids, respectively.

The film thickness h is given:

$$h(x) = h_1 - (h_1 - h_0)\frac{x}{L_1} \tag{10}$$

where h_0 is minimum film thickness, L_1 – the bearing length, and δ – the thickness of the porous matrix as shown in the fig. 1. The relevant boundary conditions for the velocity components are:

– At the upper interface ($y = H$)

$$u = U,\ v_1 = 0 \tag{11a}$$

– At the porous lower interface ($y=0$)

$$u = U,\ v_1 = 0 \tag{11b}$$

$$v = -v^* \tag{11c}$$

where v^* is the Darcy velocity component in the y-direction in the porous region.

The flow of micropolar lubricants in a porous matrix is governed by the modified Darcy's law, which account for the polar effects is given by:

$$\vec{q}^{\,*} = \frac{-\phi}{(\mu+K)}\Delta p^* \tag{12}$$

where $\vec{q}^{\,*} = (u^*, v^*)$ is the modified Darcy velocity vector:

$$u^* = \frac{-\phi}{(\mu+K)}\frac{\partial p^*}{\partial x} \tag{13}$$

$$v^* = \frac{-\phi}{(\mu+K)}\frac{\partial p^*}{\partial y} \tag{14}$$

where ϕ is the permeability of the porous matrix and p^* is the pressure in the porous region, due to continuity of fluid in the porous matrix, p^* satisfies the Laplace equation:

$$\frac{\partial^2 p^*}{\partial x^2} + \frac{\partial^2 p^*}{\partial y^2} = 0 \tag{15}$$

Solution of the problem

The solution of the eqs. (7) and (9) with the corresponding boundary conditions given in eqs. (11a) and (11b) are obtained in the form:

$$u = \frac{\frac{U}{2}\{2ym(\mu+K)\sinh(mH) + K\cosh m(y-H) + K - K\cosh(my) - K\cosh(mH)\}}{\{mH(\mu+K)\sinh(mH) + K(1-\cosh(mH))\}} + \\ + \frac{1}{(2\mu+K)}\frac{\partial p}{\partial x}\left[y^2 - Hy + \frac{KH\cosh\left(\frac{mH}{2}\right) - KH\cosh m\left(y-\frac{H}{2}\right)}{2m(\mu+K)\sinh\left(\frac{mH}{2}\right)}\right] \tag{16}$$

$$v_1 = \left[U + \frac{H}{(2\mu+K)}\frac{\partial p}{\partial x}\left\{\frac{K}{m(\mu+K)}\frac{\cosh(mH)-1}{\sinh(mH)} - \mathrm{H}\right\}\right]\cdot\left\{2H + \frac{2K}{m(\mu+K)}\frac{1-\cosh(mH)}{\sinh(mH)}\right\}^{-1}\cdot \\ \cdot\left\{\sinh(my)\left(\frac{1-\cosh(mH)}{\sinh(mH)}\right) + \cosh(my) - 1\right\} + \frac{1}{(2\mu+K)}\frac{\partial p}{\partial x}\left[\frac{\sinh(my)}{\sinh(mH)}H - y\right] \tag{17}$$

where

$$m = \left\{\frac{K(2\mu+K)}{\gamma(\mu+K)}\right\}^{1/2}$$

Substituting value of u in the integral of continuity equation:

$$\frac{\partial}{\partial x}\int_0^H u\,\mathrm{d}y + v_\mathrm{H} - v_0 = 0 \tag{18}$$

where v is the axial component of the fluid velocity in the film. The velocity component u with their expression given in eq. (16) and also using the corresponding boundary conditions given in eqs. (11a), (11b), and (18) gives the general Reynolds type equation for micropolar fluid in the form:

$$\frac{\partial}{\partial x}\left\{\frac{h_0^3}{\mu(2+\lambda)}\left[\frac{-3\lambda\overline{H}^2M+3\lambda\overline{H}\tanh(M\overline{H})+2\overline{H}^3M^2(1+\lambda)\tanh(M\overline{H})}{12M^2(1+\lambda)\tanh(M\overline{H})}\right]\frac{\partial p}{\partial x}\right\}-$$

$$-\frac{\phi}{(\mu+K)}\left(\frac{\partial p^*}{\partial y}\right)_{y=0}=\frac{U}{2}\frac{\partial H}{\partial x} \tag{19}$$

where

$$\lambda=\frac{K}{\mu},\ \overline{H}=\frac{H}{h_0},\ M=\frac{mh_0}{2},\ m=\left[\frac{K(2\mu+K)}{\gamma(\mu+K)}\right]^{1/2}$$

Using Morgan-Cameron approximation and the fact that the surface $y=h+\delta$ is non-porous [1], substituting eqs. (13) and (14) in the following continuity equation for lower porous region:

$$\frac{\partial u^*}{\partial x}+\frac{\partial v^*}{\partial y}=0 \tag{20}$$

Solving eq. (15) across porous film from $y=0$, to $y=-\delta$:

$$\int_{-\delta}^{0}\left(\frac{\partial^2 p^*}{\partial x^2}+\frac{\partial^2 p^*}{\partial y^2}\right)\mathrm{d}y=0 \tag{21}$$

$$\delta\left(\frac{\partial^2 p^*}{\partial x^2}\right)=-\left[\left(\frac{\partial p^*}{\partial y}\right)_{y=0}-\left(\frac{\partial p^*}{\partial y}\right)_{y=-\delta}\right] \tag{22}$$

Using Morgan-Cameron approximation and the fact that the surface $y=-\delta$ is non-porous [1]. Also, at the interface $p=p^*$

$$\left.\frac{\partial p^*}{\partial y}\right|_{y=0}=-\delta\frac{\partial^2 p}{\partial x^2} \tag{23}$$

Substituting this in eq. (19), the general Reynolds equation is obtained in the form:

$$\frac{\partial}{\partial x}\left\{[f(H,M)]\frac{\partial p}{\partial x}\right\}=\frac{U}{2}\frac{\partial H}{\partial x} \tag{24}$$

where

$$f(H,M)=\frac{1}{\mu}\left[\frac{h_0^3}{(2+\lambda)}\frac{-3\lambda\overline{H}^2M+3\lambda\overline{H}^2\tanh(M\overline{H})+2\overline{H}^3M^2(1+\lambda)\tanh(M\overline{H})}{12M^2(1+\lambda)\tanh(M\overline{H})}+\frac{\phi\delta}{1+\lambda}\right]$$

where δ is the porous layer thickness.

Multiplying both sides of eq. (24) by h_s and integrating with respect to h_s over the interval $-C$ to C and using eqs. (2)-(4), gives the averaged Reynolds equation in the form:

$$\frac{\partial}{\partial x}\left\{[F(h,M,\alpha^*,\sigma^*,\varepsilon^*)]\frac{\partial\overline{p}}{\partial x}\right\}=\frac{U}{2}\frac{\partial h}{\partial x} \tag{25}$$

where $E(H)=h$, $E(p)=\overline{p}$ is the expected value of the film pressure, P, and:

$$F(h,M,\alpha^*,\sigma^*,\varepsilon^*)=\frac{h_0^3}{\mu(2+\lambda)}\left[\frac{B_1+3\lambda\left(\frac{h}{h_0}+\frac{\alpha^*}{h_0}\right)C_1+D_1C_1}{12M^2(1+\lambda)C_1}\right]+\frac{\phi\delta}{\mu(1+\lambda)}$$

where

$$A_1=\frac{\varepsilon^*}{h_0^3}+\frac{\alpha^{*3}}{h_0^3}+\frac{3\alpha^*\sigma^{*2}}{h_0^3}$$

$$B_1=-3\lambda M\left(\frac{h^2}{h_0^2}+\frac{2h\alpha^*}{h_0^2}+\frac{\sigma^{*2}}{h_0^2}+\frac{\alpha^{*2}}{h_0^2}\right)$$

$$C_1=\tanh\left(\frac{Mh}{h_0}\right)+\left[1-\tanh^2\left(\frac{Mh}{h_0}\right)\right]\left[\frac{M\alpha^*}{h_0}-\frac{M^3}{3}A_1\right]$$

$$D_1 = 2M^2\,(1+\lambda)\left(\frac{h^3}{h_0^3} + \frac{3h^2\alpha^*}{h_0^3} + \frac{3h\alpha^{*2}}{h_0^3} + \frac{3h\sigma^{*2}}{h_0^3} + \frac{\varepsilon^*}{h_0^3} + \frac{3\alpha^*\sigma^{*2}}{h_0^3} + \frac{\alpha^{*3}}{h_0^3}\right)$$

Case-1: (A globular sphere model)

A porous material is filled with globular particles (a mean particle size, D_c) which is given in fig. A.

The Kozeny-Carman equation is a well-known relation used in the field of tribology to calculate the pressure drop of a fluid flowing through a packed bed of solids. This equation remains valid only for laminar flow under lubrication assumptions. The kozeny-Carman equation mimics some experimental trends and hence serves as a quality control tool for physical and digital experimental results. The Kozeny-Carman equation is very often presented as permeability versus porosity, pore size and tortuosity.

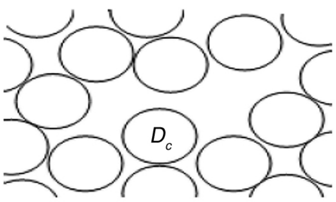

Figure A. Structure model of porous sheets given by kozeny-Carman

The pressure gradient is assumed to be linear. In view of the discussion Liu the use of Kozeny-Carman formula leads to [16]:

$$\phi = \frac{D_c^2 e^3}{72\,(1-e)^2}\,\frac{l}{l}$$

where e is the porosity and l/l' is the length ratio. Under suitable assumptions this ratio turns out to be around 2.5 from experimental results. In that case the Kozeny-Carman formula becomes:

$$\phi = \frac{D_c^2 e^3}{180\,(1-e)^2}$$

Introducing the dimensionless quantities

$$\bar{h} = \frac{h}{h_0},\ \bar{h}_s = \frac{h_s}{h_0},\ X = \frac{x}{L_1},\ P = \frac{\bar{p}h_0^2}{\mu U L_1},\ \lambda = \frac{K}{\mu},\ \alpha = \frac{\alpha^*}{h_0},\ \sigma = \frac{\sigma^*}{h_0},\ \varepsilon = \frac{\varepsilon^*}{h_0^3}$$

$$\bar{\psi} = \frac{D_c^2\delta}{h_0^3},\ \text{and}\ \bar{h} = a - (a-1)\,X$$

where $a = h_1/h_0$ and $\bar{\psi}$ is permeability parameter for Kozeny model. Equation (25) takes the form:

$$\frac{\partial}{\partial X}\left[F\,(\bar{h}, M, \alpha, \sigma, \varepsilon)\,\frac{\partial P}{\partial X}\right] = \frac{1}{2}\frac{\partial \bar{h}}{\partial X} \tag{26}$$

where

$$F\,(\bar{h}, M, \alpha, \sigma, \varepsilon) = \frac{1}{(2+\lambda)}\left[\frac{B_1 + 3\lambda\,(h+\alpha)\,C_1 + D_1 C_1}{12M^2(1+\lambda)\,C_1}\right] + \frac{\bar{\psi}e^3}{(1+\lambda)(1-e)^2}$$

$$A_1 = \varepsilon + \alpha^3 + 3\alpha\sigma^2$$

$$B_1 = -3\lambda M\,(\bar{h}^2 + 2\bar{h}\alpha + \sigma^2 + \alpha^2)$$

$$C_1 = \left\{\tanh\,(M\bar{h}) + \left[1 - \tanh^2\,(M\bar{h})\right]\left[M\alpha - \frac{M^3}{3}A_1\right]\right\}$$

$$D_1 = 2M^2\,(1+\lambda)\,(\bar{h}^3 + 3\bar{h}^2\alpha + 3\bar{h}\alpha^2 + 3\bar{h}\sigma^2 + \varepsilon + 3\alpha\sigma^2 + \alpha^3)$$

eq. (26) is dimensionless Reynolds equation.

In limiting case where porous structure, surface roughness and micropolar fluid film are absent *i.e* $\psi = 0$, $\alpha^* = \sigma^* = \varepsilon^* = 0$, $\lambda = 0$, $M = 1$, the eq. (26) reduces to the corresponding Newtonian case [17].

Since the pressure is negligible on the boundaries of the slider bearing compared to inside pressure, solving eq. (26) under conditions:

$$P = 0 \text{ when } X = 0 \text{ and } X = 1 \tag{27}$$

Integrating eq. (26) with respect to X gives:

$$\frac{\mathrm{d}P}{\mathrm{d}X} = \frac{\left(\dfrac{\bar{h}}{2} - Q\right)}{F\,(\bar{h}, M, \alpha, \sigma, \varepsilon)} \tag{28}$$

The dimensionless film pressure P is obtained as:

$$P = \int_0^X \left[F\,(\bar{h}, M, \alpha, \sigma, \varepsilon)\right]^{-1} \left[\frac{\bar{h}}{2} - Q\right] \mathrm{d}X \tag{29}$$

where

$$Q = \frac{\displaystyle\int_0^1 \frac{\bar{h}}{2F\,(\bar{h}, M, \alpha, \sigma, \varepsilon)} \mathrm{d}X}{\displaystyle\int_0^1 \frac{1}{F\,(\bar{h}, M, \alpha, \sigma, \varepsilon)} \mathrm{d}X} \tag{30}$$

The load carrying capacity, W, is given in dimensionless form:

$$W = \int_0^1 P\mathrm{d}X = -\int_0^1 X \frac{\mathrm{d}P}{\mathrm{d}X} \mathrm{d}X \tag{31}$$

Case-2: (A capillary fissures model)

In fig. B, the model consists of three sets of mutually orthogonal fissures (a mean solid size D_s) and assuming no loss of hydraulic gradient at the junctions, Irmay derived the permeability [18]:

$$\phi = \frac{D_s^2[1 - (1 - e)^{2/3}]}{12\,(1 - e)}$$

where e is the porosity.

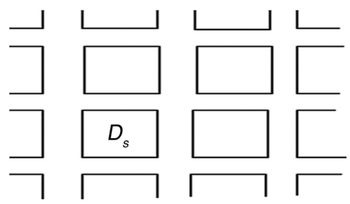

Figure B. Structure model of porous sheets given by Irmay

Considering the non-dimensional quantities:

$$G\,(\bar{h}, M, \alpha, \sigma, \varepsilon) = \frac{1}{(2 + \lambda)} \left[\frac{B_1 + 3\lambda\,(\bar{h} + \alpha)C_1 + D_1 C_1}{12M^2(1 + \lambda)\,C_1}\right] + \frac{\psi^*[1 - (1 - e)^{2/3}]}{12\,(1 + \lambda)\,(1 - e)}$$

where $\psi^* = (D_s^2\delta)\,S_h^3$ is permeability parameter for Irmay model.

Using boundary conditions (27) the dimensionless pressure distribution takes the form:

$$P = \int_0^X \left[G\,(\bar{h}, M, \alpha, \sigma, \varepsilon)\right]^{-1} \left[\frac{\bar{h}}{2} - Q\right] \mathrm{d}X \tag{32}$$

where

$$Q = \frac{\displaystyle\int_0^1 \frac{\bar{h}}{2G\,(\bar{h}, M, \alpha, \sigma, \varepsilon)} \mathrm{d}X}{\displaystyle\int_0^1 \frac{1}{G\,(\bar{h}, M, \alpha, \sigma, \varepsilon)} \mathrm{d}X} \tag{33}$$

The load carrying capacity, W, is given in dimensionless form by:

$$W = \int_0^1 P\mathrm{d}X = -\int_0^1 X \frac{\mathrm{d}p}{\mathrm{d}X} \mathrm{d}X \tag{34}$$

Results and discussion

The effect of surface roughness and micropolar lubricants on the performance characteristics of the porous inclined slider bearings is affected through the dimensionless parameters α, σ, ε, M, $\overline{\psi}$, ψ^*, e and λ. It is easily observed that the dimensionless pressure in the bearing system given by eqs. (29) and (32) while the non-dimensional load carrying capacity of the bearing system is obtained from eqs. (31) and (34). For numerical computations of the slider characteristics, the following sets of data are used for various non-dimensional parameters:

$$\lambda = 0.1, 0.2, 0.3, 0.4, e = 0.2, 0.22, 0.24, 0.26, 0.28, \alpha, \varepsilon = -0.05, -0.1, 0.0, 0.05, 0.1,$$
$$M = 4, 6, 8, 10, \sigma = 0.0, 0.1, 0.2, 0.3, 0.4, \overline{\psi}, \psi^* = 10, 20, 30, 40, 50$$

For the numerical values of the roughness parameters α, ε, σ are also chosen that the corresponding film shapes are feasible.

Pressure (Case-1)

The effect of the micropolar lubricants on the variation of the non-dimensional pressure P with X is depicted in fig. 2 for different values of permeability parameter $\overline{\psi}$. It is observed that P decreases for increasing values of $\overline{\psi}$. Figure 3 depicts the variation of P with X for different values of e. It is observed that the increasing values of e decreases the pressure. Figure 4 depicts the variation of non-dimensional pressure P with X for different values of M and it is observed that, the increasing values of M decreases pressure. It is also observed that the distribution of pressure with respect to X is significant which is seen in figs. 2 and 3.

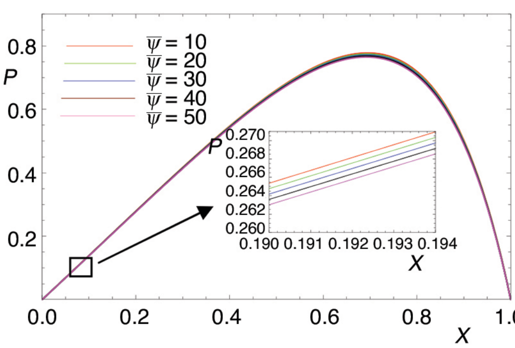

Figure 2. Variation of P with X for different values of ψ with $\alpha = -0.1$, $\sigma = 0.1$, $\varepsilon = -0.1$, $e = 0.2$, $M = 4$, $a = 2$, and $\lambda = 2$

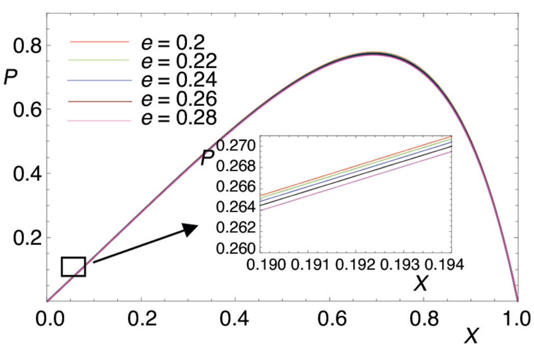

Figure 3. Variation of P with X for different values of e with $\alpha = -0.1$, $\sigma = 0.1$, $\varepsilon = -0.1$, $\overline{\psi} = 10$, $M = 4$, $a = 2$, and $\lambda = 2$

Pressure (Case-2)

The effect of micropolar fluid on the variation of non-dimensional pressure P with X for the different values of ψ^* shown in fig. 5 and it is observed that, increasing values of ψ^* decreases the pressure P. Figure 6 depicts the variation of non-dimensional pressure P with X for different values of e. It is also observed that the increasing values of e decreases the pressure P. Therefore, sharp rise in the pressure is manifested in figs. 5 and 6. In fig. 7, it depicts the variation of non-dimensional pressure P with X for different values of M and it is observed that the increasing values of M decrease pressure P.

Load carrying capacity (Case-1)

Figure 8 shows the variation of non-dimensional load carrying capacity W with λ for different values of $\overline{\psi}$. The numerical value of $\lambda = 0$ corresponds to the Newtonian case. It is

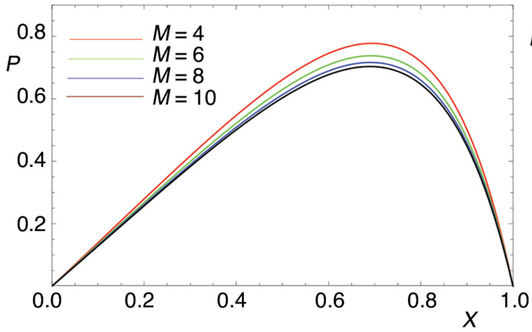

Figure 4. Variation of P with X for different values of M with α =–0.1, σ = 0.1, ε = –0.1, e = 0.2, $\overline{\psi}$ = 10, a = 2, and λ = 2

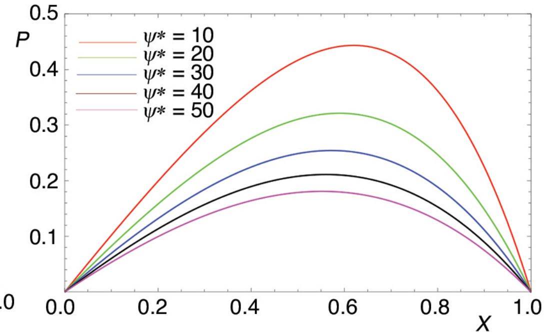

Figure 5. Variation of P with X for different values of ψ^* with α =–0.1, σ = 0.1, ε = –0.1, e = 0.2, M = 4, a = 2, and λ = 2

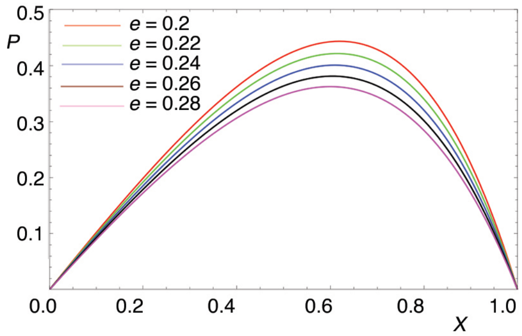

Figure 6. Variation of P with X for different values of e with α = –0.1, σ = 0.1, ε = –0.1, ψ^*= 0.2, M= 4, a = 2, and λ = 2

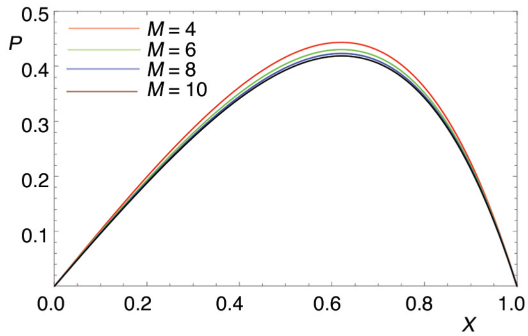

Figure 7. Variation of P with X for different values of M with α = –0.1, σ = 0.1, ε = –0.1, e = 0.2, ψ^*= 10, a = 2, and λ = 2

observed that W decreases for increasing values of λ and $\overline{\psi}$. Figure 9 shows the variation of non-dimensional load carrying capacity W with λ for different values of e and it is observed that W decreases for increasing values of λ and e. The effect of roughness parameter α, σ, and ε on the variation of W with λ is depicted in the figs. 10-12, respectively, for two values of M. It is observed that the negatively skewed surface roughness increases W whereas positively skewed surface roughness decreases W. Therefore, the significant decrease in W is observed for large values of λ as compared to the Newtonian case ($\lambda = 0$).

Load carrying capacity (Case-2)

Figure 13 shows the variation of non-dimensional load carrying capacity W with λ for different values of ψ^* and the numerical value of correspond to the Newtonian case. As λ increases load carrying capacity increases or in other words we can say that ψ^* decreases, load carrying capacity increases. Figure 14 shows the variation of non-dimensional load carrying capacity W with λ for different values of e. It has been observed that λ increases the load carrying capacity as porosity decreases. The effect of roughness parameters α, σ, and ε on the variation of W with λ is depicted in the figs.15-17, respectively, for two values of M. It is observed that negatively skewed surface roughness increases W whereas positively skewed surface roughness decreases W. Therefore significant decrease in W is observed for large values of λ as compared to the Newtonian case ($\lambda = 0$).

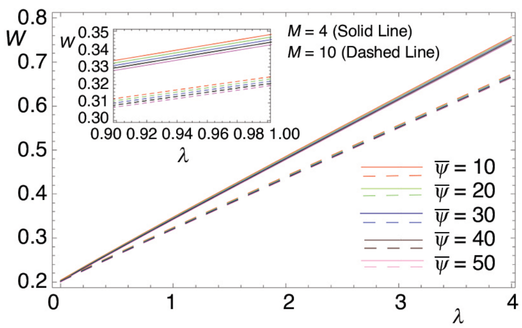

Figure 8. Variation of W with λ for different values of $\overline{\psi}$ with $\alpha = -0.1$, $\sigma = 0.1$, $\varepsilon = -0.1$, and $a = 2$

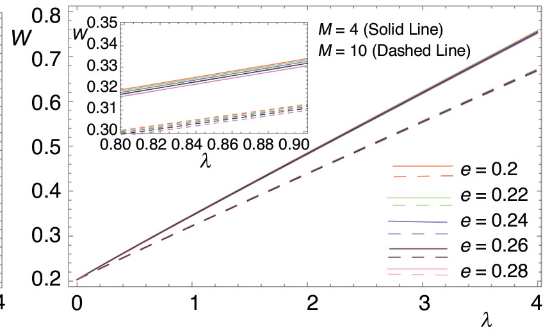

Figure 9. Variation of W with λ for different values of e with $\alpha = -0.1$, $\sigma = 0.1$, $\varepsilon = -0.1$, $\overline{\psi} = 10$, and $a = 2$

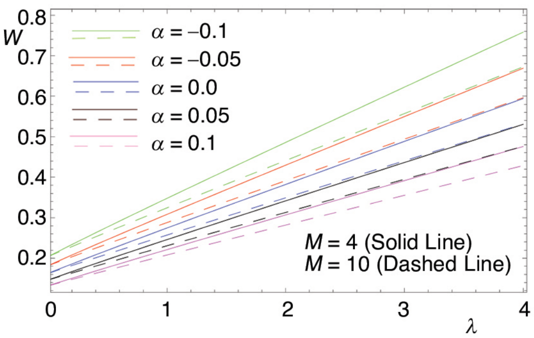

Figure 10. Variation of W with λ for different values of α with $\sigma = 0.1$, $\varepsilon = -0.1$, $e = 0.2$, $\overline{\psi} = 10$, and, $a = 2$

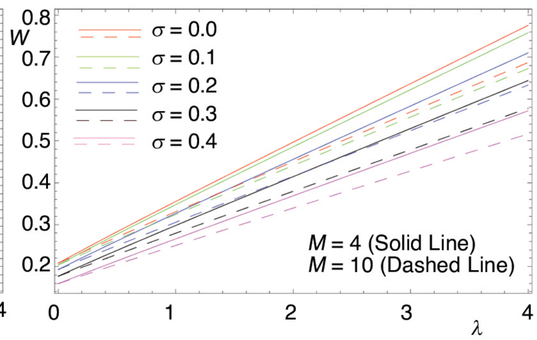

Figure 11. Variation of W with λ for different values of σ with $\alpha = -0.1$, $\varepsilon = -0.1$, $e = 0.2$, $\overline{\psi} = 10$, and $a = 2$

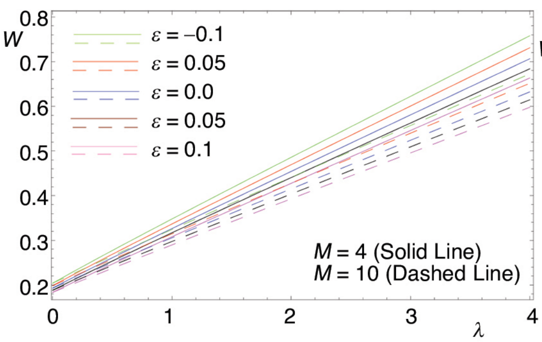

Figure 12. Variation of W with λ for different values of ε with $\alpha = -0.1$, $\sigma = 0.1$, $e = 0.2$, $\overline{\psi} = 10$, and $a = 2$

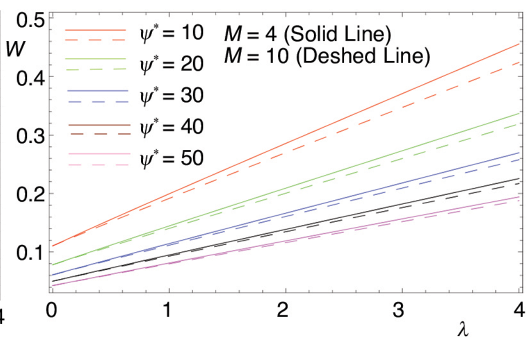

Figure 13. Variation of W with λ for different values of ψ^* with $\alpha = -0.1$, $\sigma = 0.1$, $\varepsilon = -0.1$, $e = 0.2$, and $a = 2$

Conclusions

On the basis of Christensen stochastic model, the performance of a slider bearing with surface roughness in micropolar fluid film lubrication using different porous structure have been studied. This investigation strongly suggests that the porous must be duly honoured while designing the bearing system, even if, suitable micropolar parameter is in place. Therefore, globular sphere model and Kozeny-Carman and Irmay's capillary fissures model have been subjected to investigations. A close scrutiny of the graphs suggests that the performance remains relatively better in the case of Kozeny-Carman's model as compared to Irmay's model.

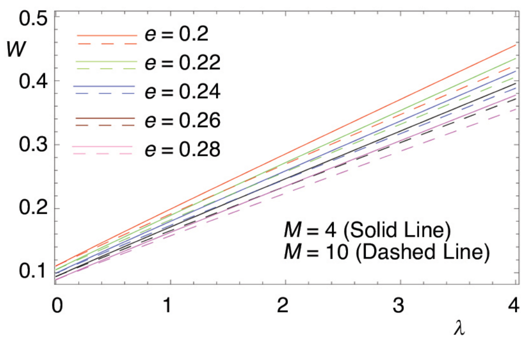

Figure 14. Variation of W with λ for different values of e with $\alpha = -0.1$, $\sigma = 0.1$, $\varepsilon = -0.1$, $\psi^* = 10$, and $a = 2$

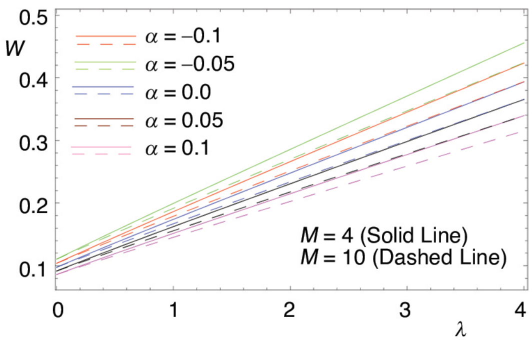

Figure 15. Variation of W with λ for different values of α with $\sigma = 0.1$, $\varepsilon = -0.1$, $\psi^* = 10$, $e = 0.2$, and $a = 2$

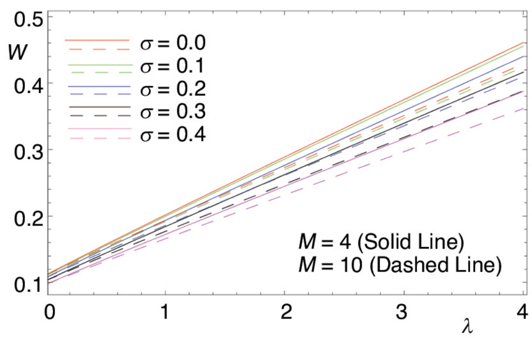

Figure 16. Variation of W with λ for different values of σ with $\alpha = -0.1$, $\varepsilon = -0.1$, $e = 0.2$, $\psi^* = 10$, and $a = 2$

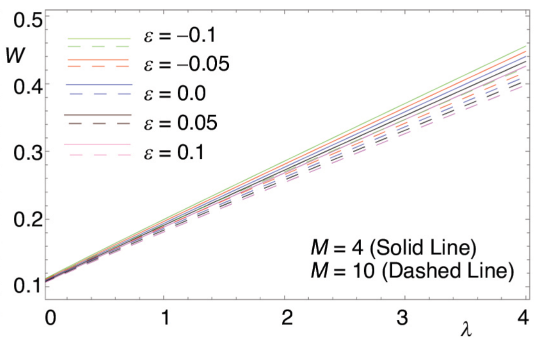

Figure 17. Variation of W with λ for different values of ε with $\alpha = -0.1$, $\sigma = 0.1$, $e = 0.2$, $\psi^* = 10$, and, $a = 2$

However, if one considers only the micropolar parameter then Irmay's model may be preferred over Kozeny-Carman's model in the case of a bearing with smooth surfaces. Also, this type of bearing systems (with the two porous structures) can support good amount of load even in the absence of flow, which is unlikely, in the case of conventional lubricants and this will open new openings in the field of tribology.

Acknowledgment

The authors wish to express sincere thanks to the Department of Applied Mathematics, Indian Institute of Technology (ISM), Dhanbad - 826004 for providing the necessary facilities. The first and third authors acknowledge financial support received from CSIR Project No. 25(0252)/16/EMR-II.

Nomenclature

C – maximum deviation from the mean film thickness
Dc – mean solid size for Kozeny model
Ds – mean solid size for Irmay model
H – film thickness
$\bar{h}$ – dimensionless film thickness $(=h/h_0)$
$h(x)$ – mean film thickness
P – dimensionless film pressure $[=(\bar{p}h_0^2)/(\mu UL_1)]$
p – lubrication film pressure
$\bar{p}$ – expected value of the lubrication film pressure $[= E(p)]$
Q – non-dimensional film thickness when P is maximum
U – sliding velocity

W – non-dimensional load carrying capacity per unit with [$= (wh_0^2)/(\mu UL_1^2)$]
X – dimensionless from of ($= x/L_1$)
x,y – cartesian co-ordinates

Greek symbols

α – non-dimensional form of ($= \alpha^*/h_0$)
α^* – mean of the stochastic film thickness
δ – porous layer thickness
ε – non-dimensional form of ($= \varepsilon^*/h_0^3$)
ε^* – measure of the symmetry of the stochastic random variable
λ – viscosity coefficient of ($=K/\mu$)
μ – classical viscosity coefficient
σ – non-dimensional form of ($= \sigma^*/h_0$)
σ^* – standard deviation of the film thickness
γ,χ – viscosity coefficients for micropolar fluids
$\overline{\psi}$ – permeability parameter for Kozeny model
ψ^* – permeability parameter for Irmay model

References

[1] Morgan, V. T., Cameron, A., Mechanism of Lubrication in Porous Metal Bearings, *Proceedings* Conference on Lubrication and Wear, Institution of Mechanical Engineers, London, 1957, pp. 151-175
[2] Uma, S., The Analysis of Double-Layered Porous Slider Bearing, *Wear*, *42* (1977), 2, pp. 205-215
[3] Prakash, J., Vij, S. K., Load Capacity and Time-Height Relations for Squeeze Films Between Porous Plates, *Wear*, *24* (1973), 3, pp. 309-322
[4] Gupta, R. S., Kapur, V. K., Centrifugal Effects in Hydrostatic Porous Thrust Bearing, *Journal of Lubrication Technology*, *101* (1979), 3, pp. 381-385
[5] Eringen, A. C., Theory of Micropolar Fluids, *Journal of Mathematics and Mechanics*, *16* (1966), 1, pp. 1-18
[6] Andharia, P. I., *et al.*, Effect of Surface Roughness on Hydrodynamic Lubrication of Slider Bearings, *Tribology Transactions, 44* (2001), 2, pp. 291-297
[7] Pinkus, O., Sternlicht, B., *Theory of Hydrodynamic Lubrication*, McGraw-Hill, New York, USA, 1961
[8] Hamrock, B. J., *Fundamentals of Fluid Film Lubrication*, McGraw-Hill, New York, USA, 1994
[9] Burton, R. A., Effects of Two-Dimensional, Sinusoidal Roughness on the Load Support Characteristics of a Lubricant Film, *ASME Journal of Basic Engineering, 85* (1963), 2, pp. 258-262
[10] Tzen, S. T., Saibel, E., Surface Roughness Effects on Slider Bearing Lubrication, *ASLE Transactions*, *10* (1967), 3, pp. 334-338
[11] Naduvinamani, N. B., Marali, G. B., Dynamic Reynolds Equation for Micropolar Fluid Lubrication of Porous Slider Bearings, *Journal of Marine Science and Technology*, *16* (2008), 3, pp. 182-190
[12] Christensen, H., Stochastic Models for Hydrodynamic Lubrication of Rough Surfaces, *Proceedings of the Institution of Mechanical Engineers*, *184* (1969), 1, pp. 1013-1026
[13] Elrod, H. G., Thin-film Lubrication Theory for Newtonian Fluids with Surfaces Possessing Striated Roughness or Grooving, *ASME Journal of Lubrication Technology*, *95* (1973), 4, pp. 484-489
[14] Prakash, J., Tiwari, K., Lubrication of a Porous Bearing with Surface Corrugations, *ASME Journal of Lubrication Technology*, *104* (1982), 1, pp. 127-134
[15] Siddangouda, A., *et al.,* Combined Effects of Micropolarity and Surface Roughness on the Hydrodynamic Lubrication of Slider Bearings, *Journal of the Brazilian Society of Mechanical Sciences and Engineering*, *36* (2014), 1, pp. 45-58
[16] Liu, J., Analysis of a Porous Elastic Sheet Damper with a Magnetic Fluid, *Journal of Tribology*, *131* (2009), 2, pp. 021801-1-5
[17] Prakash, J., Vij, S. K., Hydrodynamic Lubrication of a Porous Slider, *Journal of Mechanical Engineering Science, 15* (1973), 3, pp. 232-234
[18] Irmay, S., Flow of Liquid Through Cracked Media, *Bulletin of Research Council of Israel*, *5A* (1955), 1, 85

Paper submitted: August 25, 2017
Paper revised: December 19, 2017
Paper accepted: December 22, 2017